

## Note

# Confirmation of the D configuration of the 2-substituted arabinitol 1-phosphate residue in the capsular polysaccharide from *Streptococcus pneumoniae* Type 17F

Christopher Jones,<sup>a,\*</sup> Begoña Aguilera,<sup>b</sup> Jacques H. van Boom,<sup>b</sup> J. Grant Buchanan<sup>c</sup>

<sup>a</sup>Laboratory for Molecular Structure, National Institute for Biological Standards and Control, Blanche Lane, South Mimms, Herts EN6 3QG, UK

<sup>b</sup>Gorlaeus Laboratories, Leiden Institute of Chemistry, Leiden University, Einsteinweg 55/PO Box 9502, NL-2300RA Leiden, The Netherlands

<sup>c</sup>Department of Chemistry, University of Bath, Claverton Down, Bath BA2 7AY, UK

Received 8 April 2002; accepted 1 July 2002

Dedicated to Professor Derek Horton on the occasion of his 70th birthday

## Abstract

The absolute configuration of the 2-substituted arabinitol 1-phosphate residue present in the repeating unit of the capsular polysaccharide (CPS) from *Streptococcus pneumoniae* Type 17F is confirmed as D, based on a comparison of proton and carbon chemical shifts in a synthetic oligosaccharide and in an oligosaccharide derived from the CPS by degradation. © 2002 Elsevier Science Ltd. All rights reserved.

**Keywords:** Arabinitol; Pneumococcal polysaccharide; Vaccine; Configuration

In our recent work<sup>1</sup> reporting a refined structure and the full NMR assignments for the CPS from *Streptococcus pneumoniae* Type 17F, the absolute configuration of the 2-substituted arabinitol 1-phosphate was not independently determined, but assumed from two previous structural reports in reviews,<sup>2–4</sup> which do not contain data or information on the methodology. Given the continuing interest in the synthesis of oligosaccharides related to this CPS,<sup>5,6</sup> as a means to understand in detail the key immunological determinants,<sup>6,7</sup> it is important to provide unambiguous information on this point. The availability of synthetic material containing a 2-substituted arabinitol residue of known D-configuration **1** and an oligosaccharide from base-catalysed degradation of the CPS containing the same  $\alpha$ -L-Rha-(1→2)-arabinitol substructure, **2**, provided an opportunity to do this. The two possible substructures,

$\alpha$ -L-Rha-(1→2)-D-arabinitol **1** and  $\alpha$ -L-Rha-(1→2)-L-arabinitol **3**, are shown in Fig. 1.

For the preparation of the synthetic oligosaccharide, O-(2,3,4-tri-O-acetyl- $\alpha$ -L-rhamnopyranosyl)-(1→2)-3,4-di-O-benzyl-5-O-benzoyl-D-arabinitol was synthesised from L-Rha and D-lyxose as previously described.<sup>7</sup> Subsequent de-O-acylation under basic conditions followed by hydrogenolysis afforded the target compound **1**.

Base-catalysed degradation of the Pn17F CPS and desalting gave a hexasaccharide alditol monophosphate **2** as the ammonium salt, in which the phosphate group was distributed between the O-2 and O-3 of the terminal Rha in a ratio of approximately 1:9, due to hydrolysis of the easily formed Rha 2,3-cyclophosphate intermediate. This sample could be used for NMR studies without further purification.

Proton and <sup>13</sup>C NMR spectra for both compounds were assigned using a conventional range of techniques including TOCSY, ROESY, double-quantum filtered COSY and heteronuclear correlation methods. Proton-<sup>13</sup>C correlation spectra were optimised both for <sup>1</sup>J<sub>H,C</sub> of 150 Hz and <sup>n</sup>J<sub>H,C</sub> of 20 Hz. To avoid damage and heating effects due to extended periods of high power

\* Corresponding author. Tel.: +44-1707-654753x211; fax: +44-1707-646730

E-mail address: cjones@nibsc.ac.uk (C. Jones).

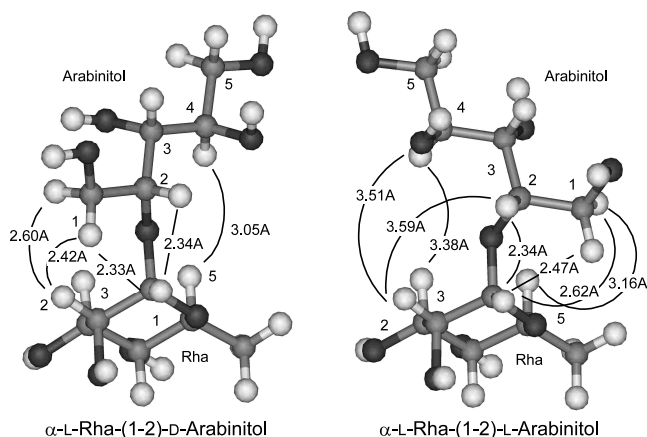


Fig. 1. Stereosketches of the structures of  $\alpha$ -L-Rha-(1 $\rightarrow$ 2)-D-arabinitol (**1**) and  $\alpha$ -L-Rha-(1 $\rightarrow$ 2)-L-arabinitol (**3**), indicating expected NOEs. Inter-atomic distances are taken from the lowest energy conformers found in the relaxed  $\phi/\psi$  map. The models were built using standard fragments and a conformation of arabinitol predicted by Angyal and Le Fur,<sup>8</sup> consistent with the inter-proton coupling constants, and energy minimised. Inter-residue inter-proton distances involving non-exchangeable protons not specifically indicated are longer than 3.7 Å.

broadband decoupling, and to ensure overlapping proton resonances could be interpreted by first order analysis, the  $^1\text{H}$ – $^{13}\text{C}$  spectra used to determine inter-proton coupling constants were obtained without  $^{13}\text{C}$  decoupling.

*Inter-proton coupling constants and the conformation of the arabinitol residue.* Inter-proton coupling constants were measured from the  $^1\text{H}$ – $^{13}\text{C}$  correlation spectrum, due to spectral overlap, and collected with high digital resolution in the proton domain. The data obtained are shown in Table 1. The close agreement between the inter-proton coupling constants for the arabinitol residue in **1** and **2** indicate that their conformations are closely similar, and as predicted by Angyal and Le Fur.<sup>8</sup> This suggests that the stereochemical analysis based on chemical shifts changes is valid, and not subject to conformational confounding factors.

*Chemical shift changes on glycosylation.* Compared to arabinitol, the corresponding  $^1\text{H}$  and  $^{13}\text{C}$  resonances in **1** and **2** are shifted, and the changes observed are very similar for both (Table 2 and Fig. 2), with a large upfield shift for C-1 (2.4 ppm), a large downfield shift for C-2 (5 ppm), and small upfield shifts for C-3 and C-4. All of the proton resonances of the arabinitol residue undergo downfield shifts, with that for the H-1s being largest. In arabinitol, and both **1** and **2**, the two H-1 resonances are coincidental. The chemical shifts of the L-Rha H-1 and C-1, which would also be expected to be sensitive to the chirality of the arabinitol residue, are also very similar in **1** and **2** (differing by 0.015 and 0.22 ppm, respectively, Table 1), although the Rha residues are differently substituted at O-4 in **1** and **2**.

Although, to the best of our knowledge, no comprehensive study of the effect on the  $^1\text{H}$  and  $^{13}\text{C}$  resonances of the alditol as a function of the relative

Table 1  
Selected proton and  $^{13}\text{C}$  chemical shifts and inter-proton coupling constants

Residue	H-1 C-1	H-1'	H-2 C-2	H-3 C-3	H-4 C-4	H-5 C-5	H-5'	H-6 C-6
D-Arabinitol	3.68 64.14	3.68	3.938 71.38	3.590 71.60	3.763 72.06	3.672 64.02	3.845	
$^3J_{\text{HH}}$	n.d.	n.d.	n.d.	9 Hz, sm	2.5, 5, 9 Hz	2.5, 12 Hz	5, 12 Hz	
<i><math>\alpha</math>-L-Rha-(1<math>\rightarrow</math>2)-D-Ara-ol (<b>1</b>)</i>								
Rha-(1 $\rightarrow$	5.051 99.16		3.999 70.95	3.805 70.61	3.461 72.29	3.840 69.54		1.285 16.97
$\rightarrow$ 2)-Ara-ol	3.804 61.68	3.804	4.007 76.30	3.714 71.32	3.732 71.78	3.690 64.11	3.828	
$^3J_{\text{HH}}$	4.5 Hz	4.5 Hz	4.5, 4.5, 1.5 Hz	1.5, 7.5 Hz	2, 4.5, 7.5 Hz	4.5, 10 Hz	2, 10 Hz	
<i>Pn17F oligo (<b>2</b>)</i>								
$\rightarrow$ 4)- $\alpha$ -Rha-	5.066		4.071	3.921	3.605	3.924		1.306
(1 $\rightarrow$	99.38		70.68	69.93	83.47	68.30		17.27
$\rightarrow$ 2)-Ara-ol	3.809 61.79	3.809	4.004 76.52	3.717 71.30	3.733 71.78	3.679 64.08	3.820	
	5 Hz	5 Hz	sm, 5, 5, Hz	sm, 9 Hz	2, 6, 9 Hz	5, 12 Hz	2, 11 Hz	

Chemical shifts referenced to internal TSP- $d_4$  at 0 ( $^1\text{H}$ ) or  $-1.8$  ppm ( $^{13}\text{C}$ ).

Table 2  
Observed glycosylation shifts compared to arabinitol

Residue	H-1 C-1	H-1'	H-2 C-2	H-3 C-3	H-4 C-4	H-5 C-5	H-5'	H-6 C-6
<i><math>\alpha</math>-L-Rha-(1→2)-arabinitol (1)</i>								
	+0.124	+0.124	+0.069	+0.124	−0.031	+0.018	−0.017	
	−2.46		+4.92	−0.28	−0.28	+0.09		
<i>Pn17F oligosaccharide (2)</i>								
	+0.129	+0.129	+0.066	+0.127	−0.030	+0.007	−0.025	
	−2.35		+5.14	−0.30	−0.28	+0.06		

Data are chemical shift of the relevant resonance in the oligosaccharide, minus that of the corresponding resonance in arabinitol.

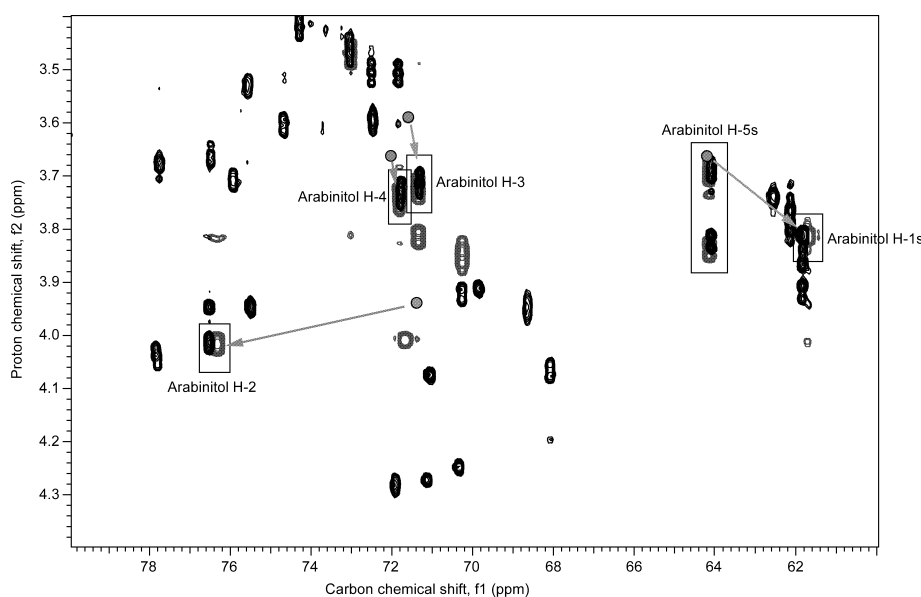


Fig. 2. Overlay of HSQC spectra of authentic  $\alpha$ -L-Rha-(1→2)-D-arabinitol (**1**) and the oligosaccharide **2** derived from the pneumococcal type 17F CPS. The pairs of resonances highlighted indicate the close similarity in chemical shifts between the D-arabinitol residue in **1** (in grey) and the arabinitol residue in **2** (in black), showing that it has the D configuration in **2**. The grey circles indicate the positions of the corresponding crosspeaks in the spectrum of D-arabinitol, and the arrows the glycosylation shifts that occur in the oligosaccharides. The H-5/C-5 and H-5'/C-5 crosspeaks of arabinitol are not shown, as they are almost coincident with the corresponding crosspeaks in **1** and **2**.

configuration of the residues has been reported for oligosaccharide alditols, such studies have been carried out for disaccharides.<sup>9,10</sup> In general, the shift of the anomeric position is either between 3 and 5 or between 8 and 8.9 ppm, depending on the configuration of the aglycone.<sup>9</sup> Similarly the glycosylated position in the aglycone ( $C_\alpha$ ) is shifted downfield (compared to the unsubstituted residue) by between 4.5 and 9 ppm, depending on the relative configurations of the sugar and the aglycone, and the anomeric configuration of the sugar. The glycosylation shifts on the  $C_\beta$  is typically upfield by between 0 and 3 ppm, with one  $C_\beta$  being shifted more than the other. Which  $C_\beta$  undergoes the larger glycosylation shift depends on a variety of stereochemical factors, including the absolute configurations of the sugar and the aglycone, the anomeric configura-

tion of the sugar, and the position of attachment of the sugar on the aglycone. The origin of these shifts on  $C_\beta$  is believed to be the interactions between protons, and is therefore similar in origin to NOEs.<sup>11</sup> There is much less data available when the aglycone is acyclic. In a  $^1\text{H}$  and  $^{13}\text{C}$  NMR study<sup>12</sup> of monosaccharide alditols of the type  $\beta$ -D-[Glc or Gal]-(1→X)-D-HexNAc-ol (where X = 3, 4 or 6, and HexNAc-ol is GlcNAc-ol, GalNAc-ol or ManNAc-ol), the shifts of  $C_\alpha$  and  $C_\beta$  were typically 7–8 ppm downfield and between 0.8 ppm downfield and 1 ppm upfield (only cases where X = 3 or 4 considered), and clearly dependent on the configuration of the alditol. Combining the  $^1\text{H}$  NMR data of Jones et al.<sup>12</sup> with that of Martensson et al.<sup>13</sup> shows that the shifts of  $H_\alpha$  and the two  $H_\beta$ s are dependent on the anomeric configuration of the sugar, and the

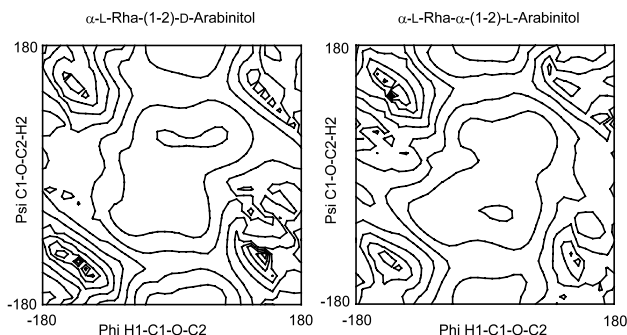


Fig. 3. Contour plots of the relaxed energy surfaces for rotation about the glycosidic linkage for  $\alpha$ -L-Rha-(1 $\rightarrow$ 2)-D-arabinitol (**1**) and  $\alpha$ -L-Rha-(1 $\rightarrow$ 2)-L-arabinitol (**3**). The contours are spaced at intervals of 5 Kcal mol<sup>-1</sup>.

configuration of the aglycone. The differences are of the order of 0.2 ppm, and should be readily distinguished by 2D NMR methods. In a study of the  $\beta$ -D-glucosides of *S*- and *R*-2-pentanol, Seo et al.<sup>14</sup> found that the <sup>13</sup>C glycosylation shifts of the pentanol C-2 differed by 2.1 ppm (9.1 vs. 7.0 ppm), and that those of the  $\beta$ -carbons were also diagnostic, depending on the absolute stereochemistry of the pentanol.

**Inter-residue NOEs and molecular modelling.** The fully relaxed  $\phi/\psi$  map of **1** (Fig. 3) shows a broad minimum at  $\psi = 50^\circ$ , between  $\phi = -10^\circ$  and  $60^\circ$ , with a secondary minimum centred around  $\phi/\psi$   $10^\circ, -50^\circ$ , approximately 1.5 kcal higher in energy. In the fully relaxed  $\phi/\psi$  map of **3**, there is a primary minimum centred at  $25^\circ, -50^\circ$ . The molecular models of the lowest energy conformers of both **1** and **3** predict

inter-residue NOEs between Rha H-1 and arabinitol H-1 and arabinitol H-2. In the ROESY spectrum of **1** (Fig. 4, bottom), a strong inter-residue NOE is observed between the Rha H-1 and the H-1s of the arabinitol residue. The other expected inter-residue NOE, to the arabinitol H-2, is obscured by overlap with the NOE and a TOCSY artefact between the Rha H-1 and H-2, but was visible in a two dimensional HSQC-ROESY experiment with a 150 ms mixing time. In the ROESY of the oligosaccharide derived from the Pn17F CPS, **2** (Fig. 3, top), the same pattern of NOEs is observed, with a strong inter-residue NOE between the Rha H-1 and the arabinitol H-1s. In this system, the NOE between the Rha H-1 and the arabinitol H-2 is clear. These NOEs do not discriminate between the two stereochemical possibilities: however, the lowest energy conformer model of **1** predicts an inter-residue NOE between the Rha H-2 and one of the arabinitol H-1s (inter-proton distance 2.42 Å), and a weak NOE between the Rha H-5 and the arabinitol H-4 (inter-proton distance 3.05 Å). The lowest energy minimum of **3**, on the other hand, predicts an inter-proton distance between Rha H-5 and arabinitol H-1 of 3.16 Å, and between Rha H-3 and arabinitol H-4 of 3.38 Å which might give rise to observable NOEs (Fig. 1). In both the ROESY and the HSQC-ROESY of **1**, observation of the first of these NOEs is obscured by an intra-residue NOEs between the Rha H-2 and H-3, and between the arabinitol H-2 and H-1: the second is obscured in the ROESY of **1**, but can be seen as a weak crosspeak at the chemical shift of Rha C-5 and arabinitol H-4. In the HSQC-ROESY spectrum of the Pn17F oligosaccharide

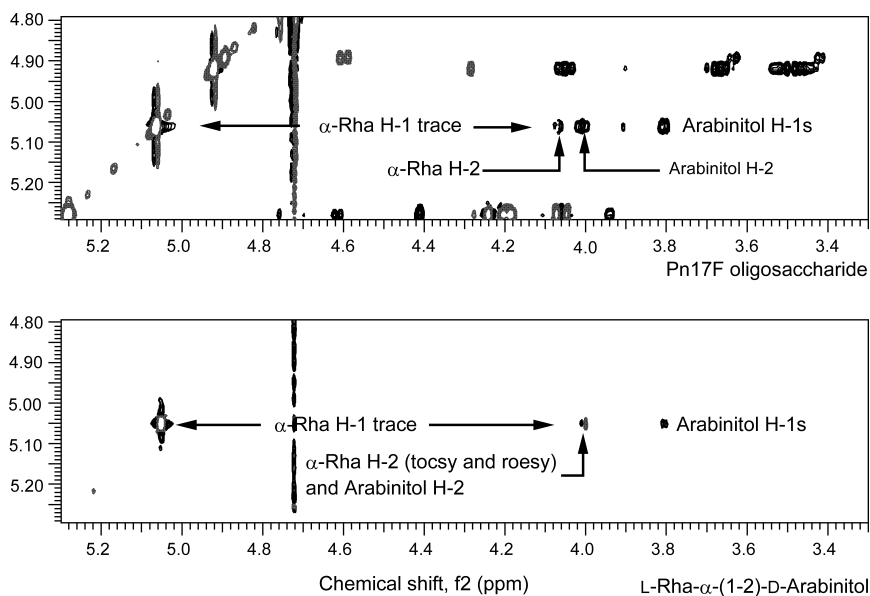


Fig. 4. Comparison of partial ROESY spectra of authentic  $\alpha$ -L-Rha-(1 $\rightarrow$ 2)-D-arabinitol (bottom), showing NOEs from the  $\alpha$ -Rha H-1 to the arabinitol H-1s. In the lower spectrum, the inter-residue NOE between the  $\alpha$ -Rha H-1 and the arabinitol H-2 is obscured by a mixed NOE and TOCSY artefact to the Rha H-2. The mixing time for both spectra was 150 ms.

**2**, obtained with a 300 ms mixing time, weak inter-residue NOEs are observed not only between the Rha H-5 and the arabinitol H-4 (observed both in the Rha C-5 and arabinitol C-4 traces), but also between the Rha H-5 and arabinitol H-2 and the H-1s. A weak NOE is observed between the Rha H-2 and the arabinitol H-1 on the arabinitol C-1 trace. The secondary minimum of **1** predicts an NOE between the Rha H-1 and the arabinitol H-4, which is not observed. Thus although NOEs diagnostic of the presence of D-arabinitol are observed, a number of unexpected ones are also seen, which may reflect the conformational flexibility of this system and the need to treat these data with caution.

**Conclusions.** Comparison of the patterns of glycosylation shifts and, less conclusively, inter-residues NOEs in an oligosaccharide derived from the Pn17F CPS **2** and authentic  $\alpha$ -L-Rha-(1 $\rightarrow$ 2)-D-arabinitol **1** indicate that the alditol in the CPS has the D configuration, confirming previous assignments. The clear-cut results reported here also rule out an alternative formulation of the 17F CPS in which the phosphate group is attached to position 5 in D-arabinitol with the  $\alpha$ -Rha attached to O-4. This possibility was not excluded in the earlier work.<sup>1</sup> It is interesting that in CPSs containing ribitol phosphate units the configuration is D-ribitol 5-phosphate<sup>15–17</sup> consistent with biosynthesis from cytidine diphosphate ribitol (CDP-ribitol).<sup>18–20</sup> If the biosynthesis of the 17F antigen follows a similar course, a nucleotide derivative of D-arabinitol 1-phosphate is indicated. In CDP-ribitol, the ribitol phosphate unit is derived from D-ribulose 5-phosphate;<sup>21</sup> a similar sequence in the D-arabinitol series might involve D-xylulose 5-phosphate.

## 1. Experimental

**General methods.**—TLC analysis was performed on E. Merck aluminium Silica Gel 60 F254 plates, with detection by charring with 20% H<sub>2</sub>SO<sub>4</sub> in MeOH. Hyflo Super Cel<sup>®</sup> was purchased from Fluka. Optical rotation was measured on a Propol automatic polarimeter (sodium D line,  $\lambda$  = 589 nm). Mass spectrometry was performed on a PE/SCIEX API 165 equipped with an ion-spray interface. Elemental analysis was carried out on a Perkin–Elmer elemental analyser.

$\alpha$ -L-Rhamnopyranosyl-(1 $\rightarrow$ 2)-D-arabinitol (**1**).—O-(2,3,4-Tri-O-acetyl- $\alpha$ -L-rhamnopyranosyl)-(1 $\rightarrow$ 2)-5-O-benzoyl-3,4-di-O-benzyl-D-arabinitol<sup>7</sup> (125 mg, 0.17 mmol) was treated with methanolic NaOMe (0.1 M, 1.7 mL) at rt for 20 h. The mixture was neutralised with Dowex-H<sup>+</sup>, filtered and concentrated. The crude compound was dissolved in MeOH (15 mL) and Pd/C (10%, 100 mg) was added. The reaction mixture was stirred under H<sub>2</sub> atmosphere for 2 h, then it was filtered

over Hyflo<sup>®</sup> Celite to avoid the particles of Pd/C passing through the filter, and concentrated. The residue was purified in several portions by gel-filtration chromatography on HW-40 (0.15 M NH<sub>4</sub>HCO<sub>3</sub> in water) to give **1** (40 mg, 76%). *R*<sub>f</sub> 0.4 (EtOAc–MeOH–water 7:2:1),  $[\alpha]_D^{25}$  –54° (c 0.2, water). ESI-MS: *m/z* = 321.0 [M + Na<sup>+</sup>]. Anal. Calcd for C<sub>11</sub>H<sub>22</sub>O<sub>9</sub>: C, 44.29; H, 7.43. Found: C, 44.06; H, 7.04.

**Degradation of the pneumococcal Type 17F CPS.**—The CPS (ca. 5 mg) was dissolved in water (200  $\mu$ L) and 40% NaOH (50  $\mu$ L) was added, and the reaction heated at 50 °C for 18 h. The base was neutralised by passage through pre-washed cation-exchange resin (BioRad AG50 1  $\times$  8, 200–400 mesh, ca. 400  $\mu$ L bed volume) in a 0.22  $\mu$  centrifugal filter. The solution was lyophilised, neutralised with ammonia and deuterium exchanged by lyophilisation from deuterated water. The one-dimensional <sup>1</sup>H NMR showed that the oligosaccharide was essentially pure and that depolymerisation was complete, with heterogeneity due to location of the phosphomonoester on either the Rha O-3 or O-2 (ratio ca. 9:1). This sample was suitable for extensive NMR analysis and spectral assignments (Table 1). A second sample, prepared from 10 mg of CPS (purchased from the American Type Culture Collection: sample prepared originally by Merck & Co.), was used for the HSQC-ROESY experiment.

**NMR spectroscopy.**—NMR spectra were obtained on either a Varian Inova 600 or a Varian Inova 500 NMR spectrometer, equipped with 5 mm inverse detection heteronuclear probes, at an indicated probe temperature of 30 °C. The software was VNMR version 6.1c. Samples were deuterium exchanged by lyophilisation prior to final dissolution in 350  $\mu$ L of deuterated water (> 99.9% <sup>2</sup>H, Aldrich) and introduction into the NMR tube (Shigemi 5 mm susceptibility matched tubes). The NMR pulse sequences used were standard Varian sequences except for the introduction of spin echo sequence into the TOCSY and ROESY experiments, and implementation of the HSQC sequence of Wider and Wüthrich for heteronuclear correlation experiments.<sup>22</sup> Inter-proton coupling constants were measured either from one-dimensional experiments or from traces of the HSQC spectra, obtained without broadband <sup>13</sup>C decoupling and with high digital resolution (ca. 0.5 Hz/point) in the proton domain. Typical parameters were (TOCSY, ROESY and COSY) to collect 4 k data points in *f*<sub>2</sub> over a 5000 Hz spectral window, zero filled to 8 k prior to Fourier transformation. 1024 increments were collected in *f*<sub>1</sub>, zero filled to 2 k prior to transformation. The mixing time for the TOCSY spectra was 80 and 150 ms for the ROESY spectra. Proton–<sup>13</sup>C correlation spectra were collected with 1500 points in *f*<sub>2</sub> and 2400 increments in *f*<sub>1</sub>, using spectra windows of 10 and 125 ppm. When high resolution was required in *f*<sub>2</sub>, 16 k data points were collected and zero filled to 32 k prior



to Fourier transformation. The HSQC-ROESY experiment was a variant of the sequence of Crouch et al.,<sup>23</sup> using the HSQC sequence of Wider and Wüthrich.<sup>22</sup> Chemical shifts are referenced to internal TSP-*d*<sub>4</sub> at 0 ppm (<sup>1</sup>H) or –1.8 ppm (<sup>13</sup>C).<sup>24</sup>

**Molecular modelling.**—Fully relaxed  $\phi/\psi$  maps were obtained for the two monosaccharide alditols **1** and **3** constructed in the INSIGHT II program and using the AMBER forcefield incorporating the modifications of Homans<sup>25</sup> for carbohydrates. The angles  $\phi$  and  $\psi$  are defined by H-1–C-1–O–C-2 and C-1–O–C-2–H-2, respectively. The maps were constructed by (i) reading an energy-minimised structure file with the L-Rha and D- or L-arabinitol residues set in conformations consistent with the inter-proton coupling constants; (ii) setting  $\phi$  and  $\psi$  to desired values (initially 0° and 0°); (iii) energy minimising the structure using the AMBER forcefield but with  $\phi$  and  $\psi$  locked; (iv) writing a full structure file; (v) reading the original structure file and repeating the procedure from (ii) using incremented values of  $\phi$  and  $\psi$ .  $\phi$  and  $\psi$  were incremented in 10° steps, so that a total of 1296 conformations were generated.

## Acknowledgements

We thank Merck & Co., Inc. for the sample of Pn17F CPS.

## References

- Jones, C.; Lemercinier, X.; Whitley, C. *Carbohydr. Res.* **2000**, *325*, 192–201.
- Perry, M. B.; Bundle, D. R.; Daoust, V.; Carlo, D. J. In *The Polysaccharides*; Kenne, L.; Lindberg, B., Eds.; Academic: New York, 1983; Vol. 2, p 287.
- Jennings, H. J. Capsular Polysaccharides as Vaccine Candidates. In *Bacterial Capsules: Current Topics in Microbiology and Immunology*; Jann, K.; Jann, B., Eds.; Springer Verlag: Berlin, 1990; p 150.
- Jennings, H. J.; Pon, R. A. Polysaccharides and Conjugates as Human Vaccines. In *Polysaccharides in Medical Applications*; Dumitriu, S., Ed.; Marcel Dekker: New York, 1996.
- Alonso de Velasco, E.; Verheul, A. F.; Veeneman, G. H.; Gomes, L. J.; van Boom, J. H.; Verhoef, J.; Snippe, H. *Vaccine* **1993**, *11*, 1429–1436.
- Jansen, W. T.; Verheul, A. F.; Veeneman, G. H.; van Boom, J. H.; Snippe, H. *Vaccine* **2001**, *20*, 19–21.
- Veeneman, G. H.; Gomes, L. J. F.; van Boom, J. H. *Tetrahedron* **1989**, *45*, 7433–7448.
- Angyal, S. J.; Le Fur, R. *Carbohydr. Res.* **1980**, *84*, 201–209.
- Kochetkov, N. K.; Chizhov, O. S.; Shashkov, A. S. *Carbohydr. Res.* **1984**, *133*, 173–185.
- Shashkov, A. S.; Lipkind, G. M.; Knirel, Y. A.; Kochetkov, N. K. *Magn. Reson. Chem.* **1988**, *26*, 735–747.
- Lipkind, G. M.; Shashkov, A. S.; Mamyan, S. S.; Kochetkov, N. K. *Carbohydr. Res.* **1988**, *181*, 1–12.
- Jones, C.; Previato, J. O.; Mendonça-Previato, L. *Carbohydr. Res.* **2000**, *328*, 321–330.
- Martensson, S.; Lvery, S. B.; Fang, T. T.; Bendiak, B. *Eur. J. Biochem.* **1998**, *258*, 603–622.
- Seo, S.; Tomita, Y.; Tori, K.; Yoshimura, K. *J. Am. Chem. Soc.* **1978**, *100*, 3331–3339.
- Branefors-Helander, P.; Erbing, C.; Kenne, L.; Lindberg, B. *Carbohydr. Res.* **1977**, *56*, 117–122.
- Qin, H.; Grindley, T. B. *Can. J. Chem.* **1999**, *77*, 481–494.
- (a) Toukach, F. V.; Arbatsky, N. P.; Shashkov, A. S.; Knirel, Y. A.; Zych, K.; Sidorczyk, Z. *Carbohydr. Res.* **2001**, *331*, 213–218;  
(b) A revised structure is reported in Zych, K.; Toukach, F. V.; Arbatsky, N. P.; Kolodziejska, K.; Senchenkova, S. N.; Shashkov, A. S.; Knirel, Y. A.; Sidorczyk, Z. *Eur. J. Biochem.* **2001**, *268*, 4346–4351.
- Baddiley, J.; Buchanan, J. G.; Carss, B. *J. Chem. Soc.* **1957**, 1869–1876.
- Shaw, D. R. D. *Biochem. J.* **1962**, *82*, 297–302.
- Glaser, L. *J. Biol. Chem.* **1964**, *239*, 3178–3186.
- Glaser, L. *Biochim. Biophys. Acta* **1963**, *67*, 525–530.
- Wider, G.; Wüthrich, K. *J. Magn. Reson.* **1993**, *102*, 239–241.
- Crouch, R. C.; McFadyen, R. B.; Daluge, S. M.; Martin, G. E. *Magn. Reson. Chem.* **1990**, *28*, 792–796.
- Wishart, D. S.; Bigam, C. G.; Yao, J.; Abildgaard, F.; Dyson, H. J.; Markley, J. L.; Sykes, B. D. *J. Biomol. NMR* **1995**, *6*, 135–140.
- Homans, S. W. *Biochemistry* **1990**, *29*, 9110–9118.